

# **DESIGN OF AN AUTOMATED ULTRASONIC SCANNING SYSTEM FOR IN-SITU COMPOSITE CURE MONITORING AND DEFECT DETECTION**

Tyler B. Hudson<sup>1\*</sup>, Frank L. Palmieri<sup>1</sup>, T. Bryce Abbott<sup>2</sup>, Jeffrey P. Seebo<sup>3</sup>, Eric R. Burke<sup>1</sup>

<sup>1</sup>NASA Langley Research Center, Hampton, VA 23681, USA

<sup>2</sup>NASA Internships and Fellowships, NASA Langley Research Center, Hampton, VA 23681, USA

<sup>3</sup>Analytical Mechanics Associates Inc., Hampton, VA 23666, USA

\*Corresponding author

## **ABSTRACT**

The preliminary design and development of an automated ultrasonic scanning system for in-situ composite cure monitoring and defect detection in the high temperature environment of an oven was completed. This preliminary design is a stepping stone to deployment in the high temperature and high pressure environment of an autoclave, the primary cure method of aerospace grade thermoset composites. Cure monitoring with real-time defect detection during the process could determine when defects form and how they move. In addition, real-time defect detection during cure could assist validating physics-based process models for predicting defects at all stages of the cure cycle. A physics-based process model for predicting porosity and fiber waviness originating during cure is currently under development by the NASA Advanced Composites Project (ACP).

For the design, an ultrasonic contact scanner is enclosed in an insulating box that is placed inside an oven during cure. Throughout the cure cycle, the box is nitrogen-cooled to approximately room temperature to maintain a standard operating environment for the scanner. The composite part is mounted on the outside of the box in a vacuum bag on the build/tool plate. The build plate is attached to the bottom surface of the box. The scanner inspects the composite panel through the build plate, tracking the movement of defects introduced during layup and searching for new defects that may form during cure. The focus of this paper is the evaluation and selection of the build plate material and thickness. The selection was based on the required operating temperature of the scanner, the cure temperature of the composite material, thermal conductivity models of the candidate build plates, and a series of ultrasonic attenuation tests. This analysis led to the determination that a 63.5 mm thick build plate of borosilicate glass would be utilized for the system. The borosilicate glass plate was selected as the build plate material due to the low ultrasonic attenuation it demonstrated, its ability to efficiently insulate the scanner while supporting an elevated temperature on the part side of the plate, and the availability of a 63.5 mm thick plate without the need for lamination.

# 1. INTRODUCTION

## 1.1 Cure Monitoring and Defect Detection in Composites

Composite materials are being used more often in aerospace structures because of their higher strength-to-weight ratio compared to metals. With their rise in popularity, a need for a rapid and inexpensive non-destructive evaluation (NDE) system for these parts is growing. Much of the focus of NDE lies in the detection of defects in composite materials from the manufacturing process prior to use and damage obtained during the service life of the structure. However, it would be beneficial to find any defects in composite materials that occur during the manufacturing process including during the cure step. For thermoset-based advanced composite materials, defects such as porosity and fiber waviness may form during the resin cure cycle. During the curing process, an exothermic polymerization reaction of the thermoset resin takes place where dense polymer networks form to strengthen the resin and transform it into an insoluble, glassy material [1]. It is important to ensure the cure reaction is uniform across the composite. If it is not, these property gradients and residual stresses can cause thermal and chemical deformation such as warpage, cracking, and delamination [1]. It is also important to allow air and volatiles to escape; otherwise, any gasses trapped in the composite create high porosity areas that decrease the strength and performance of the material [2].

There has been substantial prior research on cure monitoring techniques. Popular methods include dielectric analysis (DEA) [3] and conventional bulk wave ultrasound [4-6]. In addition, guided wave ultrasound using piezoelectric transducers [7,8] and Fiber Bragg Gratings (FBGs) [8,9] has been recently demonstrated. A detailed discussion of each technique was provided in prior publications by the authors [7-9]. However, to the authors' knowledge, defect detection, localization, and quantification during cure has not been previously demonstrated.

Cure monitoring with real-time defect detection during the process could determine when defects form and how they move. In addition, real-time defect detection during cure could assist validating of physics-based process models for predicting defects at all stages of the cure cycle. A physics-based process model for predicting porosity and fiber waviness originating during cure is currently under development by the NASA Advanced Composites Project (ACP). In addition, real-time detection during cure could inform how the temperature cycle, pressure applied, bagging scheme, and layup contribute to the formation of defects and potentially suggest mitigation techniques to avoid them.

## 1.2 Principle of Ultrasonic Pulse-Echo Scanning

Ultrasonic pulse-echo scanning is a widely used method in NDE. This technique uses a piezoelectric transducer to send ultrasonic waves through the thickness of a material. When the ultrasonic wave encounters a boundary between two media (e.g., composite-water boundary, composite-air boundary), the wave is partially reflected back to the scanning head. Using the measured amplitude and time of flight of returned waves, the size and location of the defects (e.g., voids) in the material can be determined [10]. This process works best on materials with low ultrasonic attenuation, since the ultrasonic energy must be preserved as the wave passes through the material in order to ensure a clean, measurable response.

For most applications, the scanning head is moved on or above one surface of the material being tested in a raster scan motion. This process creates a map, or C-scan image, of the material with any defects or material property changes highlighted using the reflected waves [11]. In industry, this process has traditionally been used to find defects after fabrication and during the service life of composite. This technique is especially useful for internal defects and those too small to be observed using visual inspection.

### 1.3 Proposed System

The proposed system will allow for ultrasonic scanning during the composite resin cure process to achieve both cure monitoring and defect detection. The system will consist of an X-Y raster scanner that will be located in the oven while the composite panel is being cured. Since the oven reaches a maximum temperature of around 190 °C during cure, the scanning system will be contained in a nitrogen-cooled box. The inside of the container will maintain a constant temperature of around 38 °C to preserve a controlled operating environment for the scanning system. The composite panel will be vacuum bagged to the build plate on the bottom surface of the box. The scanner will inspect the composite panel through the build plate, tracking the movement of defects introduced during layup and searching for new defects that may form during cure. This preliminary design is a stepping stone to deployment in the high temperature and high pressure environment of an autoclave, the primary method of curing aerospace grade thermoset composites. Figure 1 illustrates the general concept of the proposed system.

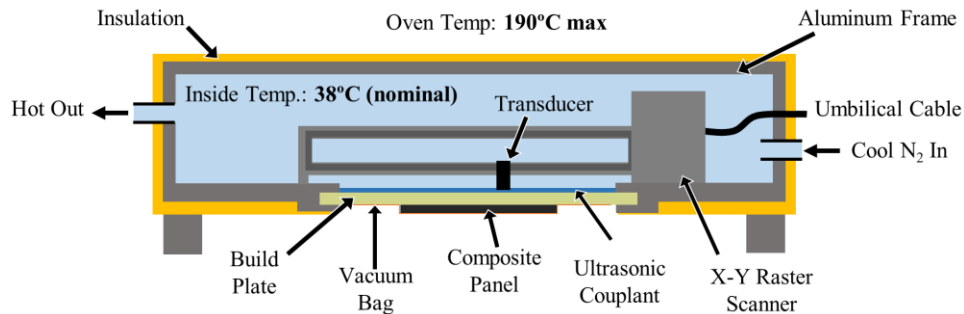


Figure 1. Proposed in-process C-scanning system for cure monitoring.

For the ultrasonic scanner to be able to inspect through the build plate into the composite panel, the material used for the build plate must have low ultrasonic attenuation. In addition, the build plate must be mechanically stiff and able to support a 38 °C to 177 °C gradient between the cooled inside of the box and the heated outside of the box. This will ensure the cure temperature of the composite part can be reached while maintaining a safe operating temperature for the scanner. The total process time of a standard cure cycle is around 6 hours for carbon fiber reinforced polymer (CFRP) composites, with a temperature hold for two hours at the maximum cure temperature of 177 °C. Therefore, the build plate must be a material with a low thermal conductivity that is able to maintain the through-thickness temperature gradient and withstand high temperatures for an extended period of time without deforming or degrading. Using a material with a low thermal conductivity allows the insulator material to be thinner, offering ultrasonic waves less resistance as they travel through the build plate into the composite and back to the transducer.

There is scarce former literature on materials that possess both low ultrasonic attenuation and low thermal conductivity. However, it may be helpful to consider the relationship between ultrasonic attenuation and elastic modulus. These two properties are directly correlated, which allows guided and bulk wave techniques to determine state of cure and transition points from wave attenuation measurements [12,13]. Baste [14] even describes a method of deriving a material stiffness matrix from wave amplitude and time of flight data. Typically, materials with high elastic moduli have lower ultrasonic attenuation. For materials with low thermal conductivity, the best insulators are highly porous materials filled with air or vacuum, but such materials would have high acoustic attenuation. Therefore, a fully dense material with low thermal conductivity was required.

Only the bottom side of the box (the one being scanned through) must have low ultrasonic attenuation; therefore, the other sides of the box can be made of a different material only considering thermal insulation. For the remaining sides, an aluminum 80/20<sup>®</sup> frame was sheathed with 38 mm thick sheets of porous, ceramic insulation (Skamol<sup>®</sup>: Skamotec 225) that have a thermal conductivity value of 0.07 W/mK.

## 2. EXPERIMENTATION

### 2.1 Candidate Materials

To determine the best material for the build plate, several materials were first chosen based on publicly available material properties. Since materials with a high modulus of elasticity typically have lower ultrasonic attenuation, high modulus materials were considered. A high elastic modulus also helped ensure a flat, undeformed build plate throughout cure. Metals are known to have low ultrasonic attenuation, but high thermal conductivity. Foams are known to have low thermal conductivity, but high ultrasonic attenuation. Because of these properties, metals and foams were determined to be an inadequate material for the bottom panel of the box. Glass is known to have low ultrasonic attenuation and a moderate thermal conductivity. Phenolic resin is known to have a low thermal conductivity and a moderate ultrasonic attenuation. Because of these properties, borosilicate glass (Swift Glass Company<sup>®</sup>), lead oxide (PbO) glass (Schott<sup>®</sup> RD-50), soda lime glass (Swift Glass Company<sup>®</sup>), and natural linen grade phenolic resin sheet with natural linen reinforcement (Interstate Plastics<sup>®</sup>) were chosen as candidate materials. The properties of these materials were confirmed with thermal conductivity models as well as ultrasonic attenuation tests that mimic the proposed setup.

### 2.2 Thermal Conductivity

The model predicts the temperature through the thickness of the tool/part at steady state during cure for different insulator materials and thicknesses (tool or part). The purpose of this model is to determine the thickness of each material required to maintain an adequate cure temperature in the composite. The temperature model is based off the system shown in Figure 2 and was derived from the relative heat flux equation represented in Eq. (1) [15]. Eq. (2) assumes the heat flux through the different panels is equal. The insulator/composite interface temperature,  $T_m$ , was calculated using Eq. (3).

$$\dot{q} = -K \left( \frac{\Delta T}{B} \right) \quad (1)$$

$$\frac{T_1 - T_m}{R_p} = \frac{T_m - T_2}{R_i} \quad (2)$$

$$T_m = \frac{R_i T_1 + R_p T_2}{R_p + R_i} \quad (3)$$

where  $\dot{q}$  is the heat flux through the thickness ( $\text{W}/\text{m}^2$ ),  $B$  is the thickness of the material (m),  $K$  is the thermal conductivity ( $\text{W}/\text{mK}$ ),  $\Delta T$  is the temperature difference across the material,  $T_1$  is the temperature in the oven,  $T_2$  is the temperature inside of the box, and  $R_{p,i}$  is thermal resistance ( $\text{m}^2\text{K}/\text{W}$ ) equal to  $B/K$  of the composite plate and insulator, respectively.

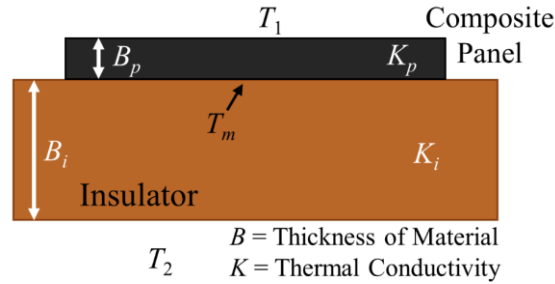


Figure 2. Diagram for temperature model ( $i$ : insulator,  $p$ : composite panel).

The model was used with the four chosen materials of varying thicknesses between 6.35 mm and 63.5 mm. For the model, the composite part with a thermal conductivity of 0.575 W/mK was chosen to be 5 mm thick, a thickness near to that of a twenty-ply panel when using 190 g/m<sup>2</sup> fiber areal weight.

## 2.3 Ultrasonic Attenuation Tests

To determine the best material with respect to ultrasonic attenuation, the ultrasonic attenuation of each proposed insulator was tested by conducting pulse-echo ultrasonic C-scans of the composite defect panels through each material. All ultrasonic C-scans were performed with a MISTRAS® UltraPAC™ Scanning Bridge Configuration fitted with a Panametrics-NDT™ Accuscan A326R 5.0 MHz/0.375 in. (9.53 mm) immersion transducer.

### 2.3.1 Composite Panel Descriptions

Four, twenty-four-ply, quasi-isotropic panels were laid up by hand from HexPly® IM7/8552 unidirectional prepreg (35% resin content, 190 g/m<sup>2</sup>) from Hexcel®. The first panel was a 305 mm × 305 mm panel and contained several planned defects. In this defect panel, four pieces of Kapton® film of different sizes were included between various layers to simulate delamination and 3M™ Glass Bubbles S22 ( $\rho = 0.22 \text{ g}/\text{cm}^3$ ) were included in various amounts between different layers to simulate porosity. The position and size of these defects are shown in Figure 3a. The percent values in Figure 3 represent the percent porosity by volume with respect to a 6 mm thick area of the composite material with a diameter of 25.4 mm. A 0.5% porosity value corresponds to 0.0034 g of glass microspheres, 1% to 0.0067 g, 2% to 0.0134 g, and 4% to 0.0268 g. The actual affected area could be larger or smaller; therefore, the percent porosity values should only be used as a reference to indicate the mass of glass microspheres introduced into the composite. A second panel

with the dimensions 114 mm × 89 mm was laid up with one square of Kapton<sup>®</sup> film and two areas of glass bubbles, all located between different layers. Figure 3b shows the position and size of these defects. Two additional panels were laid up similarly to the 114 mm × 89 mm panel. These two panels were both 102 mm × 102 mm and have identical defects. The position and size of their defects are shown in Figure 3c. The ply numbers indicate between which two plies the defect is located as counted from the bottom of the panel (i.e., ply 1 is the bottom ply and ply 24 is the top ply). Each panel was cured in an autoclave according the manufacturer’s recommended cure cycle.

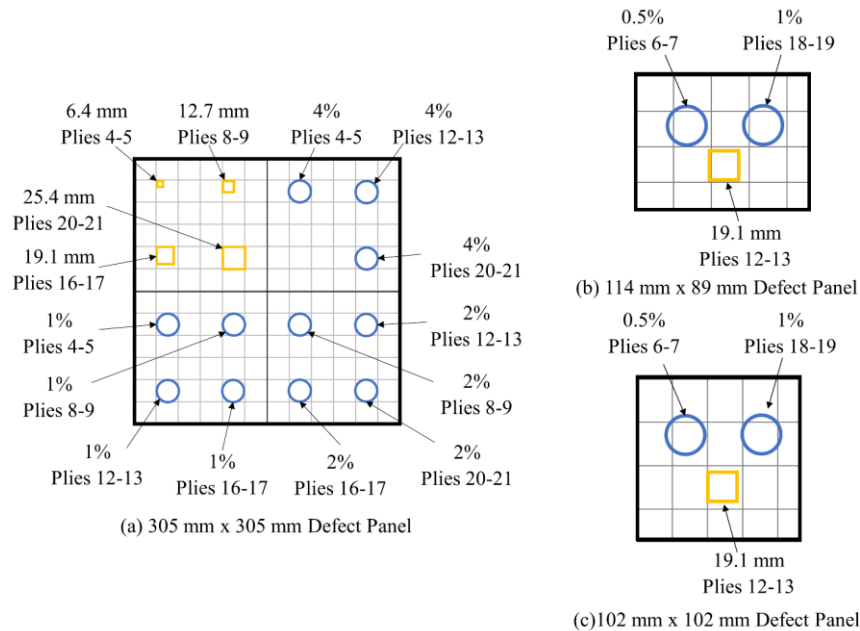


Figure 3. Defect panel layups.

### 2.3.2 Traditional Bagging Layup

The first tests simulated a traditional bagging setup, shown in Figure 4. For this test, 25.4 mm thick samples of the phenolic sheet and the soda lime glass were used separately as the build plate, and the previously cured composite defect panel was vacuum bagged to the build plate so that only fluorinated ethylene propylene (FEP) was between the insulator and the composite panel. The bagging setup was oriented in the scanner so that the ultrasonic wave would penetrate the insulator first.

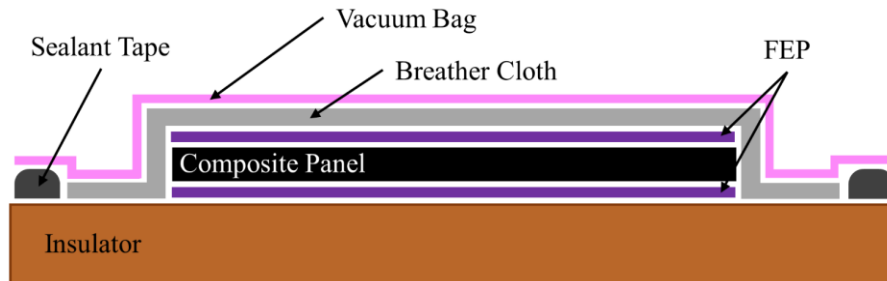


Figure 4. Bagging scheme.

### ***2.3.3 Insulator with Water Couplant***

In a second set of attenuation tests, the traditional bagging setup was simplified to investigate if penetrating both materials was possible. When submerging the panels for the ultrasonic scan, water was allowed to flow between the insulator and the composite panel to act as an ultrasonic couplant between the two panels. To ensure both plates were parallel, sealant tape was laid around the edges of the composite panel and the insulator was adhered to the other side of the tape. The tape served as a spacer and gaps in the tape lining allowed water to flow between the insulator and composite panel. This setup is shown in Figure 5. Similar to the traditional bagging scans, the setup was positioned so that the ultrasonic wave would penetrate the insulator first. The 305 mm × 305 mm composite defect panel was only tested with the phenolic sheet and soda lime glass panels because the PbO and borosilicate glass samples were too small for the large defect panel. To test the attenuation through the PbO glass, the 114 mm × 89 mm panel was used.

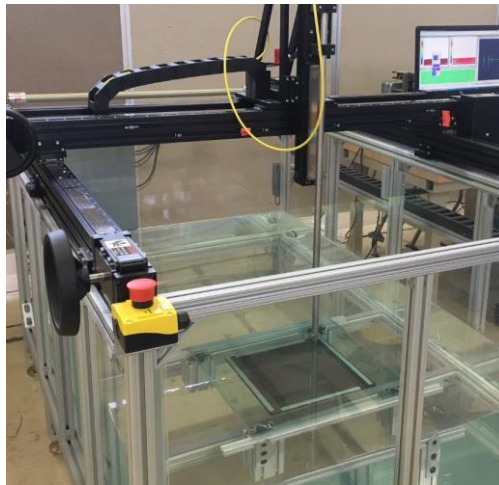


Figure 5. Water couplant setup.

### ***2.3.4 Composite Cured on Build Plate***

The first two sets of tests did not account for the flow of the resin during cure that causes the composite to conform to the build plate. Since the described system will monitor the composite during cure, this process could create the intimate contact between the composite and the insulator necessary for adequate ultrasonic penetration. In addition, Aqualene™, a solid couplant that could be utilized as a couplant during cure, was tested as a replacement for the water utilized in the previous tests. Aqualene™ would fill the air gaps between the insulator and composite panels while maintaining an ultrasonic attenuation similar to water. According to Ginzler et al. [16], Aqualene™ has an attenuation of 5 dB normalized relative to water with a 10 MHz probe operating at room temperature. This is low compared to other elastomers, including ethylene-propylene copolymer (EPDM) with a normalized attenuation of 36 dB and nitrile and neoprene with normalized attenuation values of 51 dB. Aqualene™ can be used at temperatures up to 200 °C, which meets the requirements of the proposed scanning setup in the oven. In addition, Aqualene™ is an insulator, which could further insulate the area below the composite panel.

Prior to cure, one 102 mm × 102 mm defect panel was vacuum bagged directly to the 25.4 mm thick soda lime glass panel and another was separated from the same glass panel by a 2 mm thick section of Aqualene™ solid couplant. The two panels were cured together in an autoclave per the manufacturer’s recommended cure cycle. Post cure and without removing vacuum, the two panels were scanned through the 25.4 mm thick soda lime glass plate to emulate a scan during cure.

### 3. RESULTS AND DISCUSSION

#### 3.1 Thermal Conductivity

The results of the temperature model for the candidate materials at varying thicknesses are represented in Figure 6. The input parameters for the model were a composite thickness of 5 mm, composite conductivity of 0.575 W/mK, oven temperature of 191 °C, and box internal temperature of 38 °C. The phenolic sheet was the best insulator. It maintained a 176 °C temperature at the composite with a 12.7 mm thickness. The PbO glass required a 57 mm thickness before it could support the 177 °C temperature at the composite/insulator interface. Both the soda lime glass and borosilicate glass were not able to maintain the desired gradient at the maximum 63.5 mm thickness, but they may be close enough for a proper cure. With a 63.5 mm thickness, the soda lime glass and borosilicate glass should be able to support a 173 °C and 169 °C temperature, respectively.

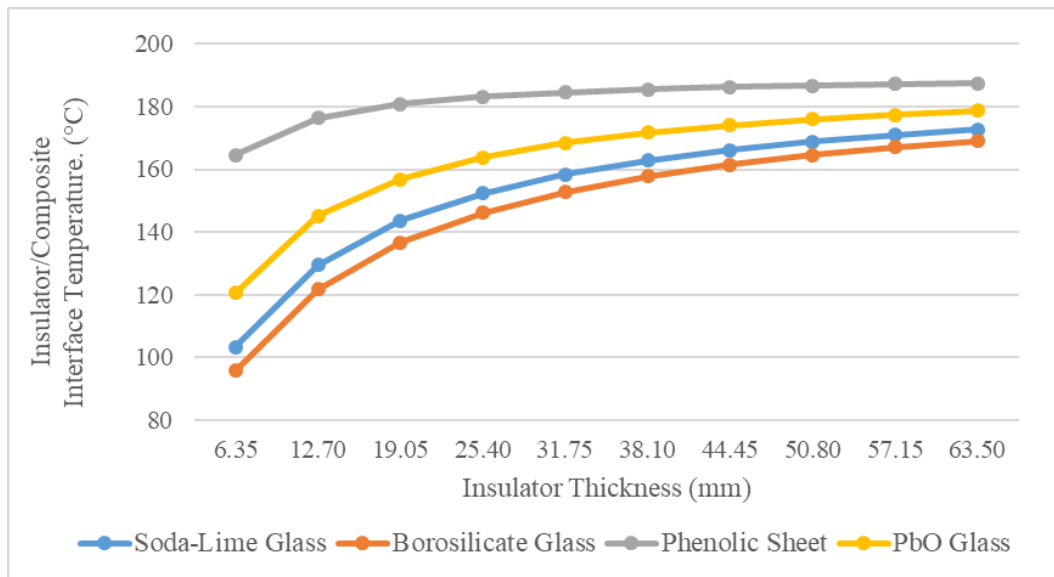


Figure 6. Results of temperature models for candidate build plate materials.

#### 3.2 Ultrasonic Attenuation Tests

##### 3.2.1 Traditional Bagging Layup

In the traditional bagging setup, the ultrasonic wave could not penetrate through the back wall of any of the insulators into the composite. Instead, the wave repeatedly reflected within the insulator. The lack of ultrasonic penetration into the composite panel could have been due to a sharp material property change between the insulators and the composite panel that resulted in a nearly-full reflection; however, it was most likely due to air trapped between the layers. Even with a small

pocket of air, the impedance mismatch between air and a solid can lead to the loss of the majority of wave energy. When silicone couplant was applied between all layers in the traditional bagging setup, the wave was able to penetrate through the insulator and composite with relatively small attenuation.

### 3.2.2 Insulator with Water Couplant

The water couplant filled any air gaps between the insulator and composite panel to allow the ultrasonic waves to penetrate into the composite panel and detect defects through 25.4 mm thick phenolic sheet and soda lime glass panels. The C-scan results are shown in Figure 7. Because the insulator/composite panel stack was flipped and oriented in the scanner so that the ultrasonic wave would penetrate the insulator first, defects on the right side of Figure 3 are on the left side of the C-scan image (Figure 7 and Figure 8) and vice versa.

The maximum amplitude plots show the highest amplitude percentage recorded through the composite panel's thickness. These plots indicate the in-plane location of any defects. The time gate/window where the maximum amplitude was calculated was just after the front surface of the composite and just before the back surface (i.e., the maximum amplitudes plotted are only from within the composite panel). Figure 7 indicates there was significantly more attenuation in the phenolic resin panel than the soda lime glass panel. The amplitude of the defects found through the phenolic resin panel were in the 4% max amplitude range, while the defects were in the 30% max amplitude range for the soda lime glass. The Kapton<sup>®</sup> film defects were also not found in the phenolic resin test, and the porosity defects found were less apparent. With a soda lime glass insulator, all defects were located.

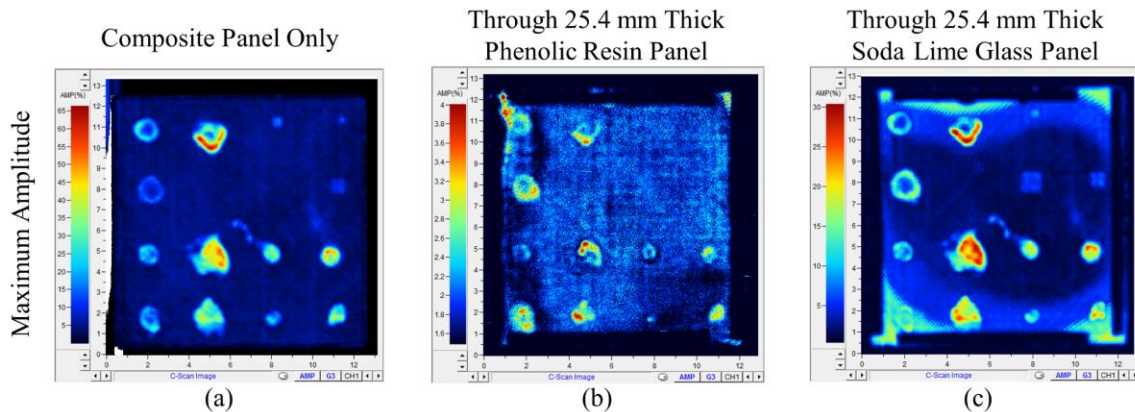


Figure 7. Ultrasonic C-scans of 305 mm × 305 mm defect panel through proposed insulators.

The C-scan images from the scan through the 7.94 mm PbO glass panel and 63.5 mm borosilicate glass panel, shown in Figure 8, revealed that both glass materials also had low attenuation, similar to the soda lime glass. 7.94 mm and 63.5 mm for PbO and borosilicate, respectively, were the thickest monolithic sheets that could be procured. Thicker glass sheets are manufactured by laminating multiple sheets together with a polymer-based adhesive. A 50 mm sample of laminated PbO glass was tested to compare to the 63.5 mm borosilicate glass, but the reflections from the laminations were too tightly spaced and interfered with the wave data from the composite panel. Of note, the 63.5 mm thick borosilicate glass panel was the last to be procured, thus the last one

tested, and incorporated improved data acquisition settings on the Mistras UT system that allowed the maximum amplitude measured from the reflections of the defects within the composite panel to be around 60% (compared to 30% for previous testing of 25.4 mm soda lime glass and 40% for 7.94 mm PbO glass). In summary, all three glass types (soda lime, PbO, and borosilicate) possessed significantly lower ultrasonic attenuation than the phenolic resin sheet and would be acceptable for use in the future system. However, the availability of non-laminated, solid 63.5 mm thick borosilicate glass, compared to 7.94 mm PbO and 25.4 mm soda lime, makes it the best option.

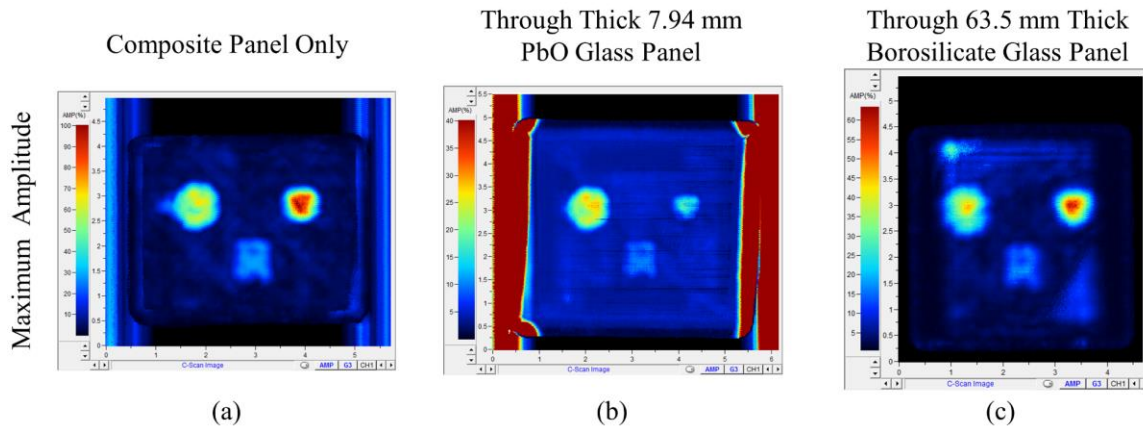


Figure 8. Ultrasonic C-Scan of 114 mm  $\times$  89 mm defect panel.

### 3.2.3 Composite Cured on Build Plate

The results for the panels cured using the 25.4 mm thick soda lime glass as the build plate, shown in Figure 9, indicated that the resin flowed and wetted the glass plate and the solid couplant, creating intimate contact between surfaces for effective defect monitoring. The air pockets at the edges likely formed after the cured part was removed from the autoclave. Loss of load from the autoclave allowed the panel to strain and slightly delaminate around the edges. Defects were detected with and without the elastomer couplant, but the couplant further reduced the area of air pockets near the edges. The maximum relative amplitude of the scan through the elastomer couplant was smaller than with no couplant, but the defects appeared clearer and there were no areas where the plate was completely obscured. The dark areas around the panels shown in Figure 9(a) and Figure 9(b) are pools of resin bleed from the composite.

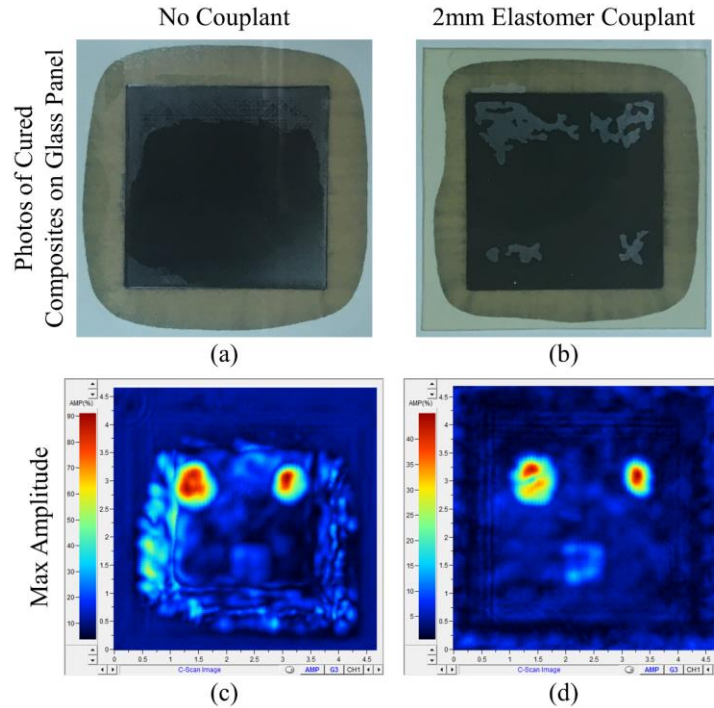


Figure 9. Ultrasonic C-scans of defect panels cured on soda lime glass.

#### 4. CONCLUSIONS

The thermal model indicated that the phenolic sheet had the best insulating properties; however, the attenuation observed in scans through the phenolic sheet indicated that a thickness large enough to reduce deformation of the sheet to an acceptable level would not allow adequate defect detection. The thermal model evaluations and attenuation tests determined that 50 mm thick PbO glass would be the best material to use for the build plate. However, a monolithic 50 mm thick PbO glass panel is not commercially available without lamination of multiple sheets. The glass laminate obscured ultrasonic inspection of the composite part. The thickest glass available without lamination was a 63.5 mm panel of borosilicate glass. All defects introduced into the composite were successfully detected and localized through the sample. A 457 mm × 457 mm × 63.5 mm borosilicate glass panel was acquired for future use in the system. It was also shown that it is possible to detect defects with the panel laid up directly to the insulating glass without the use of a couplant between the composite and the insulating build plate, though the use of an elastomer couplant improves the reliability and quality of the inspection.

#### 5. ACKNOWLEDGEMENTS

The authors would like to acknowledge Sean Britton and Hoa Luong for assistance in composite fabrication and testing.

## 6. REFERENCES

- [1] Antonucci, V., Giordano, M., Cusano, A., Nasser, J. & Nicolais, L., "Real time monitoring of cure and gelification of a thermoset matrix." *Composites Science and Technology* 66 (2006): 3273-3280.
- [2] Jeong, H., "Effects of voids on the mechanical strength and ultrasonic attenuation of laminated composites." *Journal of Composite Materials* 31 (1997): 276-292.
- [3] Nixdorf, K. & Busse, G., "The dielectric properties of glass-fibre-reinforced epoxy resin during polymerisation." *Composites Science and Technology* 61 (2001): 889-894.
- [4] Maffezzoli, A., Quarta, E., Luprano, V., Montagna, G. & Nicolais, L., "Cure monitoring of epoxy matrices for composites by ultrasonic wave propagation." *Journal of Applied Polymer Science* 73 (1999): 1969-1977.
- [5] Lionetto, F. & Maffezzoli, A., "Monitoring the cure state of thermosetting resins by ultrasound." *Materials* 6 (2013): 3783-3804.
- [6] Lionetto, F., Rizzo, R., Luprano, V. & Maffezzoli, A., "Phase transformations during the cure of unsaturated polyester resins." *Materials Science and Engineering: A* 370 (2004): 284-287.
- [7] Hudson, T. B. & Yuan, F. G., "Automated in-process cure monitoring of composite laminates using a guided wave-based system with high temperature piezoelectric transducers." *Journal of Nondestructive Evaluation, Diagnostics and Prognostics of Engineering Systems* 1 (2018): 021008.
- [8] Hudson, T.B., "Real-time Cure Monitoring of Composites Using a Guided Wave-based System with High Temperature Piezoelectric Transducers, Fiber Bragg Gratings, and Phase-shifted Fiber Bragg Gratings." *Dissertation, Doctor of Philosophy Aerospace Engineering, North Carolina State University*, (2017).
- [9] Hudson, T. B., Auwajjan, N. & Yuan, F. G., "Guided wave-based system for real-time cure monitoring of composites using piezoelectric discs and fiber Bragg gratings/phase-shifted fiber Bragg gratings." *Journal of Composite Materials* (2018): 0021998318793512.
- [10] Gholizadeh, S., "A review of non-destructive testing methods of composite materials." *Procedia Structural Integrity* 1 (2016): 50-57.
- [11] Garnier, C., Pastor, M., Eyma, F. & Lorrain, B., "The detection of aeronautical defects in situ on composite structures using Non Destructive Testing." *Composite Structures* 93 (2011): 1328-1336.
- [12] Chen, J., Hoa, S., Jen, C. & Wang, H., "Fiber-optic and ultrasonic measurements for in-situ cure monitoring of graphite/epoxy composites." *Journal of Composite Materials* 33 (1999): 1860-1881.
- [13] Stone, D. & Clarke, B., "Ultrasonic attenuation as a measure of void content in carbon-fibre reinforced plastics." *Non-destructive Testing* 8 (1975): 137-145.
- [14] Baste S., "Determination of elastic properties by an ultrasonic technique." *Proceedings of the 12th International Conference on Composite Materials, Paris*. 1999.
- [15] Balmer, R. T. *Modern engineering thermodynamics-textbook with tables booklet*. Academic Press, 2010.
- [16] Ginzler, E., Ginzler, R. & Brothers, G., "Ultrasonic properties of a new low attenuation dry couplant elastomer." *Ginzler brothers & associates Ltd* (1994).